

Modified Vertical Bridgman Growth of $\text{Cd}_{1-x}\text{Zn}_x\text{Te}$ Detector Grade Crystal in a 4 inch EDG Furnace

Amlan Datta, Kelly A. Jones, Santosh Swain, Kelvin G. Lynn, *Washington State University, Pullman, WA*

Abstract—Achieving a high yield of detector grade CdZnTe single crystals is one of the greatest challenges in CdZnTe crystal growth. Over 85, 3.5–4 inch long CdZnTe crystals were grown in a 43 zone modified low pressure Vertical Bridgman Electro-Dynamic Gradient (EDG) Freeze 3 in. Mellen Sunfire furnace. The diameter of the grown ingots has been increased using a new Electro-Dynamic Gradient (EDG) Freeze 4 in. Mellen Sunfire Platinum coil furnace to visualize the effects of increased ampoule diameter on the grain structure and spectroscopic properties of CdZnTe . The reproducibility of detector grade crystals using the 4 in. furnace is discussed and some properties of the fabricated detectors are presented.

I. INTRODUCTION

OVER the last few decades CdZnTe has emerged as a novel material for detection of soft γ -rays and hard X-rays at room temperature with high detection efficiency and sharp energy resolution. Due to the high material density (5.78 g/cm^3), average atomic number (49.1) and wide band gap (1.57 eV with 10% Zinc) [1], CdZnTe has high stopping power and low thermal noise which makes it an excellent choice as a nuclear detector at room temperature. Its high photorefractive coefficient and IR transmittance makes CdZnTe an excellent substrate for IR windows in IR cameras and devices. Stable and linear detection, operability at body temperature and high spatial resolution allows CdZnTe to be used in Digital Radiography and Nuclear Medicine detectors [2].

Due to thermal and physical properties of CdZnTe , it is extremely difficult to control the liquid-solid growth interface and maintain a desired stoichiometric composition. The stoichiometry of the CdTe solidus is severely asymmetric [3]. As a consequence it is very difficult to maintain a particular composition with accuracy. The segregation coefficient of zinc in CdZnTe varies from 1.16 to 1.35 (i.e. >1) [4] which results in inhomogeneous distribution of Zinc in both axial and radial directions. Higher ionicity results in easier formation of

vacancies [5] and dislocations. The homogeneity of the crystal not only depends on the crystallization process but also the processes that occur in the melt. According to calorimetric studies [6] full entropy is not generated during the melting which suggests that the melt is not completely disordered. Due to this short range ordering at low superheating values no supercooling occurs. Only after a critical superheating value of about 9–10K supercooling becomes considerable [7–9]. Lower superheating results in better crystal structure at the tip of the ingot.

Many growth techniques have been speculated and tried including stoichiometric and non-stoichiometric environments using Horizontal or Vertical Bridgman method, High Pressure Bridgman (HPB), Traveling – heater method (THM) etc. Over 85 CdZnTe crystals were successfully grown using Modified Vertical Bridgman Electro-Dynamic Gradient (EDG) Freeze technique. The crystals were of 2.5 in. diameter and about 3.5 in. tall. A new furnace has been set up to grow crystals of 3.4 in. diameter expecting a cost effective high yield production of detector grade CdZnTe material. To perform as a successful detector, CdZnTe should have several crucial properties. The resistivity of the material should be high enough (typically in 10^{10} ohm-cm range) to apply bias voltage so that the charge carriers can overcome the depletion region. The mobility of the carriers should be high enough for active charge collection. Except these the crystal should be free from stacking defects, Te secondary phases and dislocations. The details of the experiment and the comparison of spectroscopic properties as well as defects with the previous 3 in. crystals will be demonstrated in this paper.

II. EXPERIMENTAL SET UP

The 4in. Electro-Dynamic Gradient (EDG) Freeze Mellen Sunfire Platinum furnace is affixed to an Aluminum fixture which allows the furnace to rotate 360° along its diameter. A stepper motor manufactured by SKF actuation system helps in moving the furnace at a constant speed of 5mm/sec vertically. It makes the system user friendly while loading or unloading the ampoule. The whole set up is enclosed in a cubicle of dimensions 7ft. x 6ft. x 9ft. The furnace, power cabinet and feedback control system were devised and assembled by Mellen Company, Concord, NH.

The furnace has a total of 43 controllable heating sections. The zones are classified into two categories single coil zones and quadrant zones. Thickness of each zone is different as shown in Fig. 1. There is a S type thermocouple near each

Manuscript received November 13, 2009. The research was funded by US Department of Energy, NA-22, Contracts DE-FG52-06/27497 and DEFG52-08NA28769.

The authors are affiliated to Center for Materials Research, Washington State University, Pullman, WA-99163, USA

(Authors' Contact email ids : amlandatta4u@wsu.edu, kelly_jones@wsu.edu, swaink@gmail.com, kgl@wsu.edu)

heating element which reads out the temperature for monitoring and feedback purposes. Also there is one thermocouple at the top running 22in. inside the furnace along the furnace axis and 5 thermocouples at the bottom in the vicinity of the ampoule.

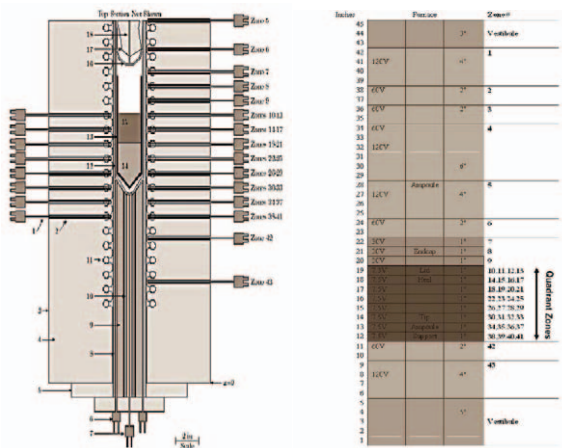


Fig. 1. Diagram on the left is the crystal growth assembly installed in the 3 in. and 4 in. furnaces with little modifications; 1 Control thermocouples, 2 Thermocouple ports, 3 stainless steel shell, 4 Alumina-silica insulation, 5 liner support, 6 four shoulder auxiliary thermocouples, 7 ampoule tip auxiliary thermocouple, 8 liner, 9 ampoule support, 10 silicon carbide tube, 11 heating coils, 12 fused silica ampoule, 13 crucible, 14 CdZnTe ingot, 15 liquid CZT, 16 ampoule cap, 17 bulk refractory fiber insulation, 18 top auxiliary thermocouple. Diagram on the right displays furnace heating zones and respective voltages applied to the heating coils.

The temperature output from the S type thermocouples advances to the 5B37 modules which are single channel signal conditioning modules that amplify the thermocouple output voltage. All of these analog values are conveyed to three 32 channel analog multiplexer board, CIO-EXP32, where 16 channels are multiplexed at each bank. An on-board semiconductor sensor provides the cold junction compensation (CJC) reference. Each CIO-EXP32 board is powered externally using a 5V DC supply. Each board yields three outputs i.e. multiplexed signals from two banks and the CJC signal which goes to the computer analog input board installed into an ISA bus slot. Any feedback and control to the system is directed from Mellen D/A64-PC analog output board to the power supply which accordingly changes the output voltage to the platinum coils. Mellen ADAPT furnace control system software is used to control the temperature setpoints which provides continuous control and feedback, Fig.2. The power supply controls the power to each heating element in the furnace using solid state relays SVDA 3V25 where load current is conducted by a SCR. An alarm system is hooked up with the total system which is triggered whenever there is a deviation from the preset parameters.

III. CHARGE PREPARATION AND GROWTH

The CdZnTe charge is composed of precompounded CdTe (6N5 purity), Zn shot (6N purity) and Te shot (6N purity) are used in proper proportions along with dopants and co-

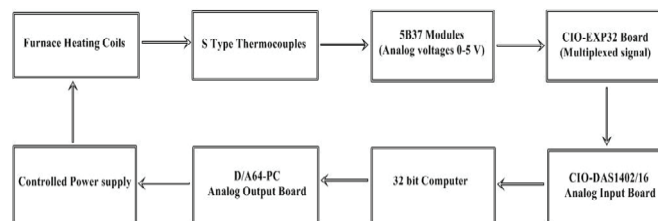


Fig. 2. Flow chart demonstrating the temperature control in the furnace.

dopants for compensation which helps in maintaining and improving the properties of the detector. 10% Zinc was added for all charges. Precompounded ZnTe and CdTe (both 6N5 purity) was used for the Pt02 charge. For Pt04 charge excess Te of 10% by weight was added. Excess Te (.3 to 10% by weight) is added to the charge, which decreases the melting temperature of the charge and prevents formation of any excess Cadmium related defects. Though it increases the supercooling (for a particular superheating value) [10], resulting in more nucleation sites and worse grain structure, it has been shown that it dramatically improves the spectroscopic properties of CdZnTe [11-13]. Excess Te also introduces deep intrinsic defects which could be compensated using a balanced doping scheme. The entire charge preparation procedure is done in a clean. The charge is then put in a GE224 quartz ampoule with pyrolytic coated graphite. An etched end cap is then placed and the ampoule is sealed at a pressure of approximately 10^{-8} Torr.

A comparison of temperature profile followed during the growth is shown in the Fig. 3. Vertical temperature gradients of 50°C and 100°C were applied after the melt growth to Pt01 and Pt02 in order to migrate Te inclusions and precipitates towards the heel region of the. Pt03 was grown at a rate of 0.55mm/hr, with an imposed gradient of 50°C/in. and was quenched during cooldown. Argon gas was flown through the furnace to reduce devitrification of quartz ampoules. The properties and grain structure of the crystals mentioned above will be compared with the 3in. furnace crystals grown in similar conditions.

IV. COMPARISON BETWEEN THE 3IN. AND 4 IN. FURNACE CRYSTALS

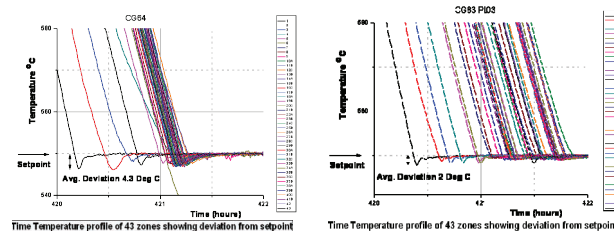


Fig. 3. Temperature vs. time. plots illustrating temperature deviation from the lower setpoints in 3 in. and 4 in. furnaces respectively.

A. Crystal Structure:

Modified Bridgman grown CdZnTe ingot mainly consists of single crystals, grain boundaries and twin boundaries. Due

to higher supercooling at the tip of the ampoule, generally in Modified Vertical Bridgman method, grain structure at the tip is worst. The grain structure is contingent upon imposed thermal conditions and material properties. The biggest single crystal cube cut from any ingot from the 3in. furnace were two 20 mm x 20 mm x 20 mm cubes whereas four such cubes can be cut from a chosen 4in. furnace grown crystal (Fig. 5). Shown in the Fig.4 are the typical grain structures of the 3 in. and 4 in. furnace for a growth under similar conditions. It is discernible that two big grains run through the whole ingot providing a high yield of single crystal from the 4in. furnace. The tip is also shown in the Fig. 5 which enables us to visualize that there are exiguous grains signifying fewer nucleation sites. It is an enormous step for optimizing the single crystal yield from a particular growth in a cost effective way. Although in one of the growths, a series of voids (fig. 4) were observed along the axis of the crystal. This may have happened because the rate of growth was too high and due to its large diameter the thermal convection was not ample for adequate mixing. The power output of the 4in. furnace is 25% higher than the 3 in. furnace. The effects of which includes higher precision in temperature control, ability to impose bigger temperature gradients and better control on the crystal growth.

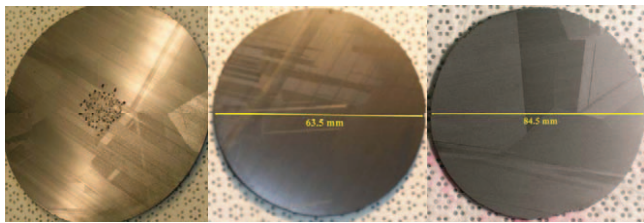


Fig. 4. The picture on left demonstrates the voids along the axial direction of the ingot in one of the 4in. furnace crystals. Middle and right side pictures show the typical grain structure of crystals grown from 3in. and 4 in. furnaces.

B. Current-Voltage characterization:

CdZnTe samples of dimensions 10mm x 10mm x 3mm are cut from single crystal regions using a diamond wire saw. As the scattering of light is dependent on the crystallographic orientation of the CdZnTe grains, recognizing clean single

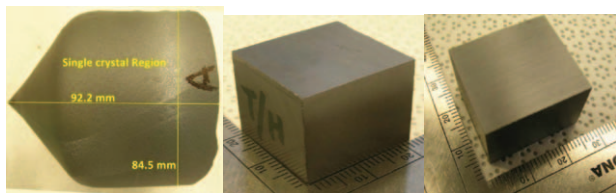


Fig. 5. Upto three 20 mm x 20 mm x 15 mm cubes could be prepared from just 2kg. charge material.

crystal region is straightforward. As samples with grain boundaries have high electron trapping cross sections, these exhibits imperfect detector properties [14, 15]. The samples are then mechanically polished using water based Alumina particle suspension to remove surface damage which degrade

the properties of a detector. Gold contacts are sputtered on opposite faces of the polished sample. The planar detectors were tested for their I-V characteristics and bulk resistivity was calculated. Average bulk resistivity value of samples from the 4 in. furnace was $2.6 \times 10^{10} \Omega\text{cm}$ compared to $2.1 \times 10^{10} \Omega\text{cm}$ which is the value for 3 in. furnace samples. The leakage current of the sample (1.48mm thick) with maximum bulk resistivity of $3.85 \times 10^{10} \Omega\text{cm}$ was 4.5 nA when 100 Volts bias was applied (Fig. 6). It is conspicuous that crystals grown in both the furnaces have comparable bulk resistivity and hence high bias voltages could be applied to collect the charge carriers.

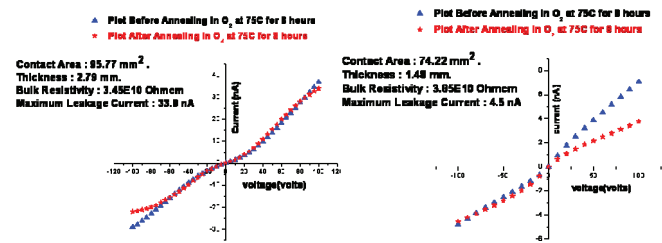


Fig. 6. Typical I-V characteristics of samples from 3 in. and 4 in. furnace respectively.

C. Radiation spectrum analysis:

A Multi-Channel Analyzer is used for spectroscopic analysis of various sources using CdZnTe. The set up of the experiment is shown in the Fig. 7. The planar detectors are connected to eV550 preamplifier using a sample holder with a beryllium window. The source is kept at a distance of 14 mm parallel to the sample. A bias voltage is applied to the sample using a Keithley high voltage source. The pulser connected to the system generates a reference pulse which is compared to the voltage pulses from the preamplifier to obtain information about the incoming radiation and background noise. Canberra Genie 2K software is used to monitor and analyze the data received from the Tennesse TC 244 shaping amplifier via Canberra 8713 analog to digital converter. The Peak to Valley ratio of the 122KeV peak from Co-57 gamma radiation spectrum of a 4 in. furnace grown planar detector shown in the Fig. 8 is 3.14 with a resolution of about 7.1%. Another detector grown in the 3in. furnace under similar conditions has a resolution of 12% with a peak to valley ratio is 2.58. The visibility of the 14 keV low energy peak depends on the background noise engendered from poor surface quality, the electrical circuit and connections, charge trapping centers etc. 14keV peaks are visible in both the cases (fig. 8) as the samples are fully depleted. Average peak to valley ratio for the 4 in. furnace is 2.3 compared to 1.8 for the 3 in. furnace. For 59.5keV gamma rays the 4 in. furnace and 3 in. furnace planar detectors has a Peak-to-Valley ratios of 20.66 and 28.5 respectively. The resolution of the 3 in. furnace cube is 6.5% whereas the resolution of the 4 in. furnace cube is 6.3%. The standard deviation on the other hand is 0.9% for the 4 in. furnace which shows that 4 in. furnace crystals are more uniform (Fig. 9).

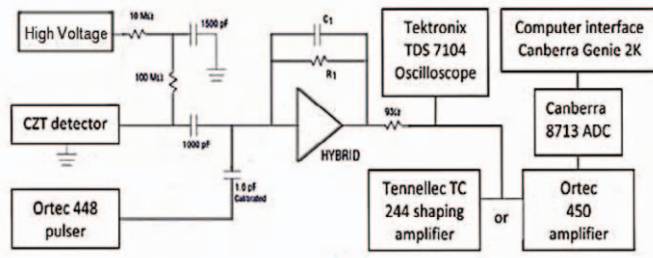


Fig. 7. Schematic diagram demonstrating the set up for Radiation Spectrum analysis of planar CZT detectors.

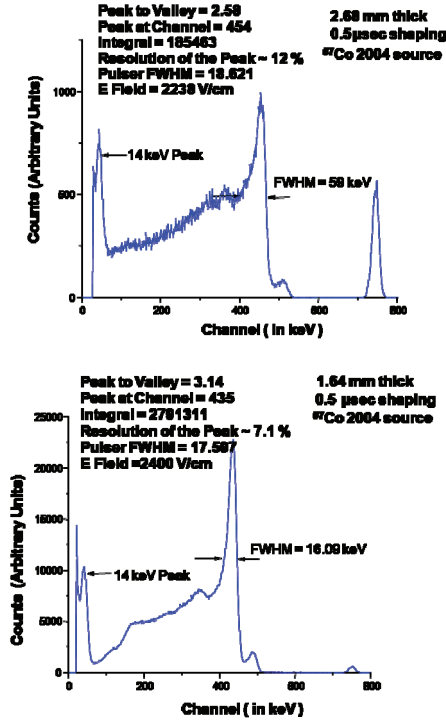


Fig. 8. Typical Co-57 Gamma Radiation Spectrum from 3in. and 4in. furnace planar detectors respectively.

D. Mobility-Lifetime product Analysis:

Mobility-lifetime product ($\mu\tau$) value reflects the potential device thickness, uniformity and efficiency of the charge carriers in the radiation detection process. The larger the $\mu\tau$ product of the charge carriers the better would be the spectroscopic properties of the detector. For the planar detectors, $\mu\tau$ values of electrons were established from Hecht relation [16], after neglecting hole contribution,

$$Q = Q_0[\mu_e\tau_e (E/D)] [1-\exp(-D/(\mu_e\tau_e E))] \quad (1)$$

where Q_0 and Q are the total initial charge generated by the incoming radiation and the collected charge respectively, E is

the applied electric field across the detectors, D is the thickness of the planar detector. In a conventional planar detector both electrons and holes contribute to the induced charge, but due to low mobility and high trapping cross section of holes (which also causes the tailing in the radiation

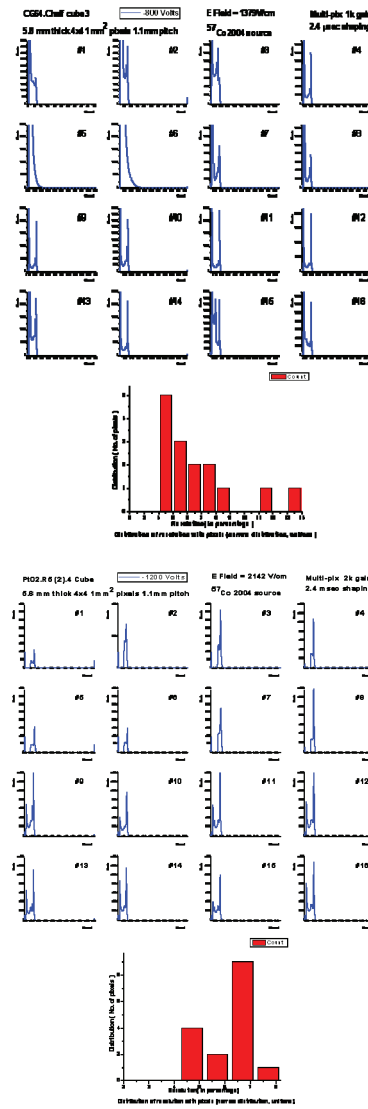


Fig. 9. ^{57}Co Spectra of a 4x4 pixilated detector from 3 in. and 4 in. furnaces respectively. Narrow distribution displays uniformity of 4 in. furnace crystals.

peaks), they are considered to be poor carriers. To neglect hole contribution in a planar device and use the Hecht relation, an excitation energy was chosen to interact near the cathode end of the device.

The collected charge (peak centroid) can be plotted against the applied electric field will give us the $\mu\tau$. The carrier generation statistics, electronic noise, non uniform charge trapping by intrinsic defects, scattering from Tellurium inclusions and other structural anomalies, Schottky barrier between the gold contact and CdZnTe, ADC linearity and detector surface conditions are some of the factors influencing the charge collection (value of Q) and hence the $\mu\tau$ value. For the pixilated cubes a contemporary approach was used [17] in which centroids (N_1, N_2) measured at two different voltages (V_1, V_2) gives us the $\mu\tau$ values using the equation,

$$\mu_e\tau_e = [D^2 / \ln(N_1/N_2)] [(1/V_1) - (1/V_2)] \quad (2)$$

The comparison of the $\mu_e\tau_e$ values at 3 μ sec shaping time and different excitation energies are compared in table I. It is evident that the detectors have comparable $\mu_e\tau_e$ for both low energy and high energy radiation sources. At room temperature without any electronic correction these values show promising carrier properties as a detector. $\mu_e\tau_e$ values as high as $1 \times 10^{-2} \text{ cm}^2/\text{V}$ have been achieved at 3 μ sec shaping time with a 3 in. furnace detector (Fig. 10). Though this kind of high value hasn't yet been achieved using the 4 in. furnace crystals, the 10^{-3} range $\mu_e\tau_e$ values depicted by the 4 in. furnace planar detectors proves that the reproducibility of crystals with good spectroscopic properties is definitely possible. The variation of $\mu_e\tau_e$ values from the pixilated detector in the radial direction is of the order of $0.05 \times 10^{-3} \text{ cm}^2/\text{V}$ proving the uniformity of the crystal. Although when the $\mu_e\tau_e$ values are compared among the detectors made from different axial positions of the ingot, a noticeable variation is observed accounted by an increase in Te secondary phases and non uniformity in crystal structure near the heel. Also, the concentration of undesired impurities, dopants and zinc [18] are inhomogeneously distributed along the length of the crystal depending on their segregation coefficient.

E. Defect Analysis :

The most consequential native defects in CdZnTe crystals are Te precipitates and inclusions. Precipitates are formed via solid state diffusion in the solid CdZnTe matrix during the cooldown due to retrograde solubility of excess Te in the non-stoichiometric solid composition. Whereas, inclusions are formed by capture of excess liquid Te droplets at the solid-liquid growth interface with morphological instabilities. Typically, the size of Te precipitates and inclusions in CdZnTe are in 10-30nm and 1-50 μ m range respectively [19].

Table I. Comparison of the $\mu\tau_e$ values of 9 mm x 9 mm x 2 mm planar detectors fabricated from both 3in. and 4in. furnace.

Crystal growth designation	5.5 MeV Am241 Alpha Source	59.5 keV Am241 Gamma Source	32.1 keV Cs137 X-Ray (Ba-K α 1 line) Source
CG51 (3in. furnace)	$1.4 \times 10^{-3} \text{ cm}^2/\text{V}$	$1.9 \times 10^{-3} \text{ cm}^2/\text{V}$	$2.3 \times 10^{-3} \text{ cm}^2/\text{V}$
CG64 (3in. furnace)	$2.4 \times 10^{-3} \text{ cm}^2/\text{V}$	$2.6 \times 10^{-3} \text{ cm}^2/\text{V}$	$3.1 \times 10^{-3} \text{ cm}^2/\text{V}$
Pt02(4 in. furnace)	$1.5 \times 10^{-3} \text{ cm}^2/\text{V}$	$2.2 \times 10^{-3} \text{ cm}^2/\text{V}$	$4.8 \times 10^{-3} \text{ cm}^2/\text{V}$

CdZnTe is transparent in the near infrared region of the radiation spectrum making IR microscopy a suitable technique for the analysis of internal defects which scatters or absorbs the IR light. IR spectroscopy is performed on a single crystal CdZnTe region using Olympus BX51M Microscope and 881 nm IR source to study the size and distribution of the Te inclusions. Image Pro Software is used to count and measure

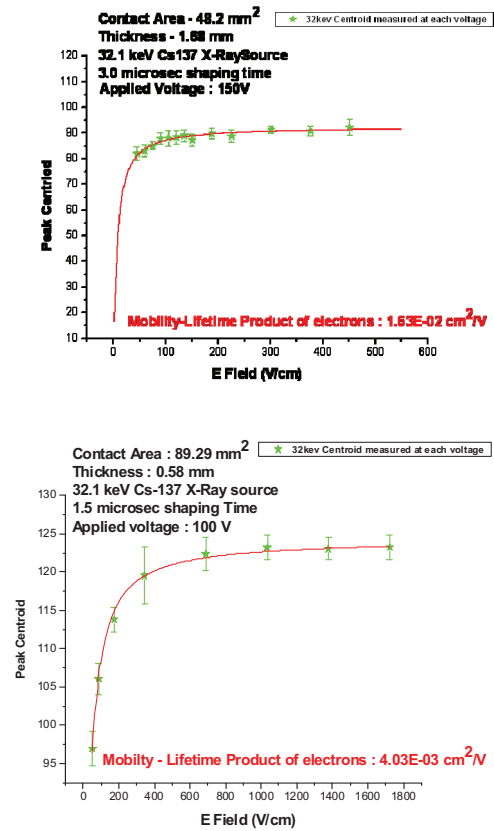


Fig. 10. Best $\mu_e\tau_e$ values from the 3 in. and 4 in. furnaces.

the diameters of the inclusions in a particular area of interest. A comparison of the Te inclusion properties is shown in table II between the best ingot of the 3 in. furnace and a typical ingot of the 4 in. furnace.

Though a volume percent as low as 0.0004% has been achieved with a 2mm thick 3 in. furnace planar detector but with the 4 in. furnace the minimum volume percent of Te inclusions achieved is 0.002% (Fig. 11). This fact accounts for not attaining $10^{-2} \text{ cm}^2/\text{V}$ range $\mu\tau$ values from the planar detectors prepared with 4 in. furnace crystals. The average values of secondary phases from both furnaces are $5.5 \times 10^{-3}\%$ and $4.0 \times 10^{-3}\%$ from 3 in. and 4 in. furnace respectively. Impurities also affect the spectroscopic quality of the detectors. They may introduce deep (Ti, Fe, V, Ni) or shallow (Au, Cu, Ag, Pb, Cr, Co) energy levels, thereby trapping more of the charge carriers causing poor resolution and low $\mu_e\tau_e$. The impurity gettering effect of Te inclusions generates high local concentration of trapping centers which worsen the detectors [20]. Impurities like Na decreases the resistivity of the CZT detectors which results in failure to use it as a radiation detector. Samples from different sections of the ingot were tested for impurities using Glow Discharge Mass Spectroscopy (GDMS) by National Research Council, Canada. In the 4in. furnace growths we managed to reduce the amount of total impurities (excluding dopants and C, N, O) to 100 ppb which is comparable to the minimum value (88 ppb) of 3in. furnace.

REFERENCES

- [1] eV Products Website, http://www.evmicroelectronics.com/pdf/material_prop.pdf
- [2] C. Scheiber, G. C. Giakos, "Medical Applications of CdTe and CdZnTe detectors," *Nuclear Instruments & Methods in Physics Research A*, Vol. 458, pp. 12-25, 2001.
- [3] J.H. Greenberg, "P-T-X phase equilibrium and vapor pressure scanning of non-stoichiometry in CdTe," *Journal of Crystal Growth*, Vol. 161, pp. 1-11, 1996.
- [4] Hans J. Scheel, Tsuguo Fukuda, "Crystal Growth Technology," *John Wiley and sons inc.*, 2003.
- [5] C. Vérié, "Beryllium substitution-mediated covalency engineering of II-VI alloys for lattice elastic rigidity reinforcement," *Journal of Crystal Growth*, Vol. 184-185, pp. 1061, 1998.
- [6] A. Amzil, Jean-Claude Mathieu, R. Castanet, "Calorimetric investigation on the Cd-Te binary alloys," *Journal of Alloys and Compounds*, Vol. 256, pp. 192, 1997.
- [7] P. Rudolph, M. Mühlberg, "Basic problems of vertical Bridgman growth of CdTe," *Materials Science and Engineering: B*, Vol. 16, pp. 8, 1993.
- [8] L. Shcherbak, P. Feichouk, O. Panchouk, "Effect of CdTe "postmelting", " *Journal of Crystal Growth*, Vol. 161, pp. 16, 1996
- [9] L. Shcherbak, "Pre-transition phenomena in CdTe near the melting point," *Journal of Crystal Growth*, Vol. 197, pp. 397, 1999.
- [10] P. Rudolph, H.J. Koh, N. Schäfer, T. Fukuda, "The crystal perfection depends on the superheating of the mother phase too — experimental facts and speculations on the "melt structure" of semiconductor compounds," *Journal of Crystal Growth*, Vol. 166, pp. 578-582, 1996.
- [11] M. Chu, S. Terterian, D. Ting, R.B. James, M. Szawłowski, G.J. Visser, "Effects of p/n Inhomogeneity on CdZnTe Radiation Detectors," *Proc. SPIE*, Vol. 4784, pp. 237, 2003.
- [12] X.Zhang, Z. Zhao, P. Zhang, R. Ji, Q. Li, "Comparison of CdZnTe crystals grown by the Bridgman method under Te-rich and Te-stoichiometric conditions and the annealing effects," *Journal of Crystal Growth*, Vol. 311, pp. 286-291, 2009.
- [13] C. Muren, S. Terterian, D. Ting, C. C. Wang, J. D. Benson, J. H. Dinan, R. B. James, A. Burger, "Effects of excess tellurium on the properties of CdZnTe radiation detectors," *Journal of Electronic Materials*, Vol. 32, No. 7, pp. 778, 2003.
- [14] C. Szeles, "CdZnTe and CdTe materials for X-ray and gamma ray radiation detector applications," *phys. stat. sol. (b)*, Vol. 241, No. 3, pp. 783-790, 2004.
- [15] P. N. Luke, E. E. Eissler, "Performance of CdZnTe Coplanar-Grid Gamma-Ray Detectors," *IEEE Transactions on Nuclear Science*, Vol. 43, No. 3, pp. 1481, June 1996.
- [16] K. Hetch, *Z Physik*, Vol. 77, pp. 235, 1932.
- [17] P. Rudolph, "Non-stoichiometry related defects at the melt growth of semiconductor compound crystals - a review," *Crystal Research and Technology*, Vol. 38, Issue 7, pp. 542-554, 2003.
- [18] P. Capper, J.E. Harris, E.S. O'keefe, C.L. Jones, "Macro- and microsegregation of Zn in bridgman-grown CdZnTe," *Advanced Materials for Optics and Electronics*, Volume 5, Issue 2, pp. 101-108, 1995.
- [19] C. Szeles, S. E. Cameron, Jean-Olivier Ndap, W. C. Chalmers, "Advances in the Crystal Growth of Semi-Insulating CdZnTe for Radiation Detector Applications," *IEEE Transactions on Nuclear Science*, Vol. 49, No. 5, pp. 2535, 2005.
- [20] G. Yang, A. E. Bolotnikov, Y. Cui, G.S. Camarda, A. Hossain, R.B. James, "Impurity gettering effect of Te inclusions in CdZnTe single crystals," *Journal of Crystal Growth*, Vol. 311, pp. 99-102, 2008

Table II. Comparison of Tellurium inclusion analysis between detectors fabricated from both 3in. and 4in. furnace.

Region (Typical Ingot)	Average diameter (microns) (4in./3in.)	Total % Volume of inclusions (4in./3in.)	Total Number of inclusions , cm ⁻³ (4in./3in.)
At the shoulder	3.65/3.15	4.8 x10 ⁻³ / 4.0 x10 ⁻³	2.95 x10 ⁵ / 1.04 x10 ⁵
Below shoulder	3.8/2.5	6.0 x10 ⁻³ / 6.3 x10 ⁻³	2.57 x10 ⁵ / 2.00 x10 ⁵
Mid ingot edge	4.66/3.69	3.7 x10 ⁻³ / 4.0 x10 ⁻³	1.05 x10 ⁵ / 6.03 x10 ³
Mid ingot Area	4.1/3.45	7.1 x10 ⁻³ / 3.1 x10 ⁻³	1.9 x10 ⁵ / 7.00 x10 ⁵

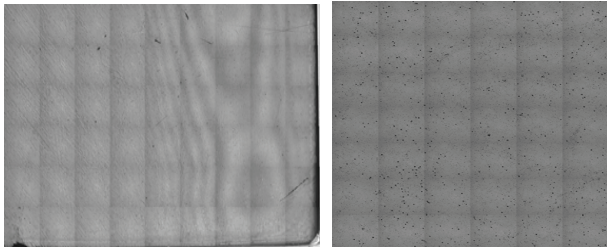


Fig. 11. IR picture at the left is of a 4.5 mm x 3mm x 1.5 mm planar detector from the 3 in. furnace with very low volume percent of inclusions (0.0004%). This detector revealed high $\mu_c\tau_c$ as shown before in Fig. 10 which clarifies the degradation of the spectroscopic properties of the detectors. The other IR picture is a region from the 4 in. furnace detector with Te inclusion percent volume of 0.002 %.

V. CONCLUSION:

The 4 in. furnace provides a higher power output resulting in uniform and precise thermal gradients which in turn leads to a better crystal structure. As a result, the single crystal detector grade CdZnTe yield from the 4 in. furnace is considerably higher. The detection properties of the samples were comparable to the 3 in. furnace samples. With high purity charge material, proper electronic compensation and suitable temperature profile, it is therefore possible to get a high yield of detector grade crystals in a 4 in. EDG Modified Vertical Bridgman Furnace. Our future goals involve growing crystals with reduced secondary phases and higher Mobility-Lifetime product values.

ACKNOWLEDGMENT

The authors thank DOE NA-22, Contracts DE-FG52-06/27497 and DEFG52-08NA28769, for their support of this research.